Food Chemistry: X 24 (2024) 101915

Contents lists available at ScienceDirect

Food Chemistry: X

journal homepage: www.sciencedirect.com/journal/food-chemistry-x

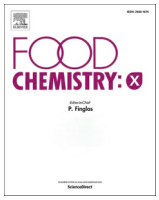

Effect of four highland barley proteins on the retrogradation and *in vitro* digestion properties of highland barley starch

Jiaxin Li [a,1], Ran Lin [a,b,1], Mengzi Nie [a], Aixia Wang [a], Xue Gong [a], Lili Wang [a], Liya Liu [a], Bin Dang [c], Xijuan Yang [c], Fengzhong Wang [a,*], Li-Tao Tong [a,*]

[a] *Institute of Food Science and Technology, Chinese Academy of Agricultural Sciences/Key Laboratory of Agro-Products Processing, Ministry of Agriculture, Beijing 100193, China*

[b] *Tianjin Key Laboratory of Food Biotechnology, School of Biotechnology and Food Science, Tianjin University of Commerce, Tianjin 300134, China*

[c] *Qinghai Tibetan Plateau Key Laboratory of Agric-Product Processing, Qinghai Academy of Agricultural and Forestry Sciences, Xining 810016, China*

ARTICLE INFO

Keywords:
Highland barley starch
Highland barley protein
Retrogradation
In vitro digestion

ABSTRACT

This study evaluated the effects of four highland barley proteins (HBPs), namely albumin, globulin, gliadin and glutenin, on the retrogradation and *in vitro* digestion properties of highland barley starch (HBS). The results showed globulin had the most significant effect on inhibiting short-term retrogradation of HBS, which was reflected in the reduction of G' and G". Compare with HBS, four HBPs could significantly inhibit long-term recrystallization process. For albumin, globulin, gliadin and glutenin, the degree of retrogradation reduced from 51.55 % to 48.20 %, 35.06 %, 42.22 % and 32.63 %, respectively, which was reflected in the decrease of water migration rate, crystal enthalpy, crystallinity and short-range order. It could be found that glutenin had the most significant effect on inhibiting long-term retrogradation of HBS. Moreover, the anti-digestion properties of retrograded HBS with HBPs intervention significantly increased, with glutenin most significantly. Compared with HBS, resistant starch (RS) content increased by 59.76 % at 28 d of retrogradation.

1. Introduction

Highland barley starch (HBS) is the main carbohydrate in highland barley grains, comprising 47.9–79.0 % of the total weight (Zhu, 2017). It serves not only an energy source in the human diet but also plays a significant functional role because of its low digestibility (Yang et al., 2022). However, starchy foods are prone to retrogradation, which negatively affects their sensory attributes and texture over time, reducing product shelf life and consumer satisfaction—posing a considerable challenge for food industries (Chen, Wang, Fan, Yang, & Chen, 2019). Over the past half-century, people have done a lot of research on starch retrogradation, not only because it significantly impacts on the quality of starchy foods, but also due to its role in regulating blood sugar levels. This is because the disordered starch could form an ordered state gradually after thermal gelatinization (Chen et al., 2019). The retrograded starch belongs to RS3 type resistant starch, also referred to as recrystallized resistant starch, which forms through the recrystallization of gelatinized starch during cooling or low-temperature storage process, resulting a dense crystalline structure. This structure hinders enzyme molecules from accessing the binding sites, thereby impeding enzymatic action easily, which might reduce the glycemic index (Chang, Zheng, Zhang, & Zeng, 2021). Therefore, it is essential to explore modification methods thant can balance the effects of HBS retrogradation on texture and its anti-digestive properties, thereby enhancing the quality and nutritional function of HBS.

Protein is the highest content of macromolecular organic matter in cereals except for starch and plays an important role in providing essential amino acids for the human body. The interaction between protein and starch during food processing significantly influences the physiochemical properties of starch, including its gelatinization, retrogradation, and digestibility (Pang et al., 2022). This interaction involves various non-covalent forces such as hydrogen bonding, electrostatic forces, van der Waals forces, and hydrophobic interactions (Lu, Donner, Yada, & Liu, 2016). Specifically, protein can form network structures during starch gelatinization process, which limit the expansion of starch granules and promote the formation of high-density structural starch-protein aggregates. These aggregates can inhibit starch retrogradation. Furthermore, protein would block the α-amylase binding site and thus

* Corresponding authors.
E-mail addresses: wangfengzhong@caas.cn (F. Wang), tonglitao@caas.cn (L.-T. Tong).

[1] Jiaxin Li and Ran Lin indicates that they are both co-first authors of this manuscript.

https://doi.org/10.1016/j.fochx.2024.101915
Received 13 July 2024; Received in revised form 7 September 2024; Accepted 20 October 2024
Available online 23 October 2024

reducing the rate of starch digestion (Bravo-Nunez, Garzon, Rosell, & Gomez, 2019). For example, the recombinant gluten components have been shown to effectively inhibit the retrogradation of wheat starch (Kuang et al., 2022). Similarly, rice protein has been observed to interfere the rice starch gelatinization, thus reducing the retrogradation degree (Wu et al., 2023) and *in vitro* digestibility (Khatun, Waters, & Liu, 2020). On other hand, whey protein has the ability to delay starch hydrolysis through the physical barrier effect (Yang, Zhong, Douglas Goff, & Li, 2019). In conclusion, elucidating the mechanism by which proteins interact with starch to inhibit starch retrogradation and induce slow starch digestion provides a deeper understanding of improving the functional properties of starchy food, which may enhance the quality of starchy foods and enrich the theoretical basis of hypoglycemic food production.

Current research on the interaction between proteins and HBS primarily focuses on exogenous proteins (Fan, Guo, & Zhu, 2022; Li et al., 2024; Yang, Wang, Zhang, Jiao, & Jin, 2024) or a specific single barley protein (Gao, Hu, Yang, Jin, & Jiao, 2024). However, highland barley protein (HBP) itself is an important nutrient component in highland barley, second only to starch in content, with significant nutritional value and bioactivity, which can be divided into four isolates: albumin, globulin, gliadin and glutenin according to the solubility. There is currently limited research exploring the interaction between HBPs and HBS in depth and the comparison among the four proteins. The HBPs may act as a retrogradation inhibitor and have anti-digestion property. Such studies would be beneficial in further understanding why highland barley products have long been considered anti-digestive and low-GI foods. Moreover, this research could help in the development and enhancement of the nutritional value and shelf stability of HBS-based food.

In this study, HBS and HBPs were used as the base materials to prepare composite gels, the effects of HBPs on the retrogradation properties and structure of HBS were investigated, and the possible mechanisms of HBS-HBPs interactions in composite gels were explored. In addition, the digestibility of retrograded HBS was determined by the *in vitro* digestion method. This study will contribute to the value-added application of highland barley components, and provide theoretical guidance for improving the quality, shelf life and functional characteristics of highland barley starch foods.

2. Materials and methods

2.1. Materials

The proteins and starch used in this study were extracted from highland barley seeds (Kunlun 15) grown in Qinghai, China. Cellulase (S10042, ≥400 U/mg) (Yuanye Technology Co., Ltd., Shanghai, China), Xylanase (DH19326, ≥6500 U/g) (Novozymes Biotechnology Co., Ltd., Tianjin, China), α-amylase (Sigma, 10 U/mg, from porcine pancreatic), pancreatin (4 × USP activity, Sigma P1750) and pepsin (Sigma, 400 U/mg, from porcine gastric mucosa) (Sigma Aldrich Trading Co., Ltd., Shanghai, China) were purchased. The total starch kits and amylose kits (Megazyme International Ireland Ltd., Wicklow, Ireland), the D-glucose assay kit (GOPOD Format, Megazyme) (Solarbio Technology Co., Ltd., Beijing, China) were purchased. The reagents and chemicals used in the tests were of all analytical grades and provided from local dealers.

2.2. Extraction of highland barely starch

HB seeds were milled to highland barley flour (HBF) and passed through a 100-mesh sieve. HBS was extracted using a double-enzyme method following the method of Nie et al. (Nie et al., 2023). 50 g of HBF was added to 300 mL of distilled water, followed by the addition of 25 mg of cellulase and 1.54 g of xylanase. The mixture was incubated in a water bath at 50 °C for 8 h. After centrifugation at 4500 rpm for 15 min, the upper yellow impurities were scraped off, leaving the lower white precipitate. The precipitate was washed three times with deionized water and then washed three times with ethanol. It was then dried at room temperature for 24 h and sifted through a 100-mesh sieve to obtain HBS. The total starch content and amylose content of obtained HBS were determined by Megazyme kits. The total starch and amylose content were 91.36 % (*w*/w) and 23.54 % (w/w), respectively.

2.3. Extraction of highland barley proteins

The four HBPs were extracted regarding the method of Tavano et al. (Tavano et al., 2022). Defatted HBF and 20 g/L NaCl solution (1:25 *w/v*) were mixed and stirred in a water bath (45 °C, 2 h) and then centrifuged (4500 rpm, 20 min).

(1) Extraction of albumin and globulin: the supernatant was dialysed in deionized water (4 °C, 48 h). It was then centrifuged (4500 rpm, 20 min) to obtain the globulin precipitate and albumin supernatant, respectively. The supernatant was then adjusted to the isoelectric point (pH 4.5) and centrifuged (4500 rpm, 20 min) to obtain the albumin precipitate.

(2) Extraction of gliadin and glutenin: the initial precipitate and 75 % ethanol solution (1:25 *w/v*) were stirred in a water bath (45 °C, 2 h) and centrifuged (4500 rpm, 20 min), and then the supernatant was rotary evaporated to obtain the gliadin; the precipitate was stirred (45 °C, 2 h) with 0.1 mol/L NaOH solution (1:25 w/v) and centrifuged (4500 rpm, 20 min). The supernatant was adjusted to the isoelectric point (pH 4.8) to precipitate glutenin. Finally, the four HBPs were freeze-dried and placed at −20 °C for subsequent experiments. The crude protein content was determined by the Kjeldahl method, and the contents of albumin, globulin, gliadin and glutenin were 80.2 %, 83.2 %, 86.2 % and 86.1 %, respectively. The molecular weight of four HBPs were determined using an Agilent 1260 Infinity high-performance liquid chromatography (HPLC) system, equipped with a multi-angle laser light scattering detector (Wyatt DAWN HELEOS II) and a differential refractive index detector (Wyatt Optilab Rex). The chromatographic separation was performed using Wyatt WTC-030S5 and WTC-010S5 columns, with molecular weight ranges of 5000–125,000 and 100–10,000, respectively. The mobile phase consisted of 0.1 mol/L Na_2SO_4, 0.1 mol/L pH 6.7 NaH_2PO_4-Na_2HPO_4, with 0.05 % NaN_3 and 0.1 % SDS. The four HBPs were dissolved in the mobile phase solution (5 mg/mL), filtered through a 0.45 μm microfilter membrane and injected with a sample volume of 20 μL. The flow rate was set at 0.2 mL/min, and the column temperature was maintained at 25 °C.

2.4. Preparation of retrograded starch gels

The four extracted HBPs were mixed with HBS in ratios of 0:100 and 10:90 (*w*/w), respectively. The mixture was dispersed in deionized water to make an 8 % suspension, which was homogenized for 30 min at room temperature and then stirred in a water bath at 95 °C for 30 min for pasting. The resulting pasted starch gels were cooled at room temperature and then was put in a 50 mL centrifuge tube, tightened the lid and placed it in a 4 °C refrigerator for retrogradation to keep the starch gel in a closed environment and isolated from external pollution, after storing at 4 °C for 1, 7, 14, 21 and 28 d, part of the retrograded gels was used to measure some gel characteristics, such as rheology, hardness, moisture distribution, and part of gels were frozen-dried, ground and sifted through a 100-mesh sieve (150 μm), the powder was kept to measure other indicators, such as thermodynamic properties, crystalline structure, digestive properties and so on.

2.5. Dynamic viscoelastic measurements

The fresh pasted gel was immediately transferred to a rheometer (Physica MCR 301, Anton Paar GmbH, Austria) set at 25 °C, using a plate and plate geometry (diameter of 50 mm, and gap of 1 mm). The storage modulus (G'), loss modulus (G"), and loss tangent (tan δ, G"/G') of the

samples were measured by dynamic scanning at an angular frequency of 0.1–10 rad/s in the linear viscoelastic region (0.1 % strain) (Kong, Zhu, Zhang, & Zhu, 2020).

2.6. Differential scanning calorimetry (DSC)

A differential scanning calorimeter (DSC 8000, PerkinElmer, Norwalk, CT, USA) was used to measure the thermal properties of HBS and HBS/HBPs mixtures. Each sample (3 mg) was mixed with 6 μL of distilled water, placed in a crucible, sealed and equilibrated at 4 °C for 1 d. The samples were heated from 30 °C to 110 °C at a heating rate of 10 °C/min. The onset temperature (T_O), peak temperature (T_P), conclusion temperature (T_C) and the enthalpy of gelatinization (ΔH_g) were recorded. The gelatinized samples were stored at 4 °C for 1, 7, 14, 21 and 28 d for retrogradation treatment, then reheated, and the enthalpy of retrogradation (ΔH_r) was recorded. The caculation and fitting for the degree of retrogradation (DR%) was performed using Eqs. (1) and (2):

$$\mathrm{DR}\ (\%) = \frac{\Delta H_r}{\Delta H_g} \times 100 \tag{1}$$

$$X(t) = \frac{\Delta H_t - \Delta H_0}{\Delta H_\infty - \Delta H_0} = 1 - exp(-kt^n) \tag{2}$$

where $X(t)$ and ΔH_t are the retrogradation degree of crystallized amylopectin and the enthalpy change stored at 1, 7, 14, 21 and 28 d, respectively; ΔH_0 is the enthalpy change at 0 d, generally regarded as zero; ΔH_∞ is the limiting enthalpy change, which was 28 d for all samples; k is the rate constant; and n is the Avrami exponent.

2.7. Low-field nuclear magnetic resonance (LF-NMR)

The water mobility in retrograded gels was evaluated through the LF-NMR analyzer (NMI20-015 V, Niumag Electric Corporation, China). The fresh pasted gels (3 mL) were poured into 10 mL glass transparent vials with screw caps and then stored at 4 °C for 1, 7, 14, 21 and 28 d, and the relaxation curves were obtained using the CPMG pulse sequence. The relaxation time (T_2) and corresponding relative peak area (A_2) were recorded (Zhang, Lin, Lei, & Zhong, 2020).

2.8. Hardness analysis

The hardness of retrograded gels stored at 4 °C for 14 and 28 d was measured by a texture analyzer (TAXT plus, Stable Co., England) with a P/0.5 cylinder probe. The pre-test, test, and post-test speed were set at 1.0 mm/s, with a strain of 50 %, an automatic trigger mode, and a trigger force of 5 g.

2.9. X-ray diffraction (XRD)

The retrograded gels stored at 4 °C for 14 and 28 d were freeze-dried and ground to further analyze the crystalline structure by an X-ray diffraction instrument (D8 Advance, Bruker, Germany) according to the previous studies with minor modifications (Zhang, Sun, Wang, Wang, & Zhou, 2020). Diffractograms were obtained over the range of 4–40 ° (2θ) at a constant rate of 4 °/min and relative crystallinity was calculated by selecting and fitting procedure using MDI Jade 6 software (Materials Data Inc., Livermore, CA) using the following Eq. (3):

$$\text{Relative crystallinity}\ (\%) = \frac{Ic}{Ic + Ia} \times 100 \tag{3}$$

where I_c and I_a indicate the peak areas of the crystalline and amorphous phases, respectively, and the detailed method was shown in the supplementary material.

2.10. Fourier-transform infrared spectroscopy (FTIR)

Freeze-dried retrograded starch powders were thoroughly ground with solid KBr powder at a mass ratio of 1:100 (*w*/w) and then pressed into sheets. Spectra were recorded over a range of 400–4000 cm^{-1} and each sample was scanned 64 times by a Fourier transform infrared spectrometer (TENSOR 27, Germany) with a resolution of 4 cm^{-1}. The 1100–950 cm^{-1} band was analyzed using the OMNIC 8.2 software (Thermo Fisher Scientific Inc., USA) for baseline correction, smoothing and Fourier deconvoluted and the absorbance ratios at 1047/1022 cm^{-1} and 995/1022 cm^{-1} were calculated (Wan et al., 2023).

2.11. Scanning electron microscope (SEM)

The retrograded gels stored at 4 °C for 14 and 28 d were freeze-dried, cross sections were cut, fixed to the sample stage with conductive tape and sputtered with gold. Cross-sections of the sample were observed at 10 kV accelerating voltage and 150 × magnification using an SEM (SU8010, Hitachi, Japan) (Zhang, Chen, Chen, & Chen, 2019).

2.12. In vitro digestion

In vitro digestion experiments were performed by the method of Nie et al. (Nie et al., 2023). The ground freeze-dried retrogradation sample (50 mg) was dispersed in 2 mL of distilled water with 3 glass spheres and 1 mL of α-amylase (50 U/mL), which was shaken for 2 min at 37 °C, then 5 mL of 400 U/mL pepsin solution was added and shaken in a water bath (37 °C, 30 min, 300 rpm). Then 5 mL 0.02 M NaOH, 20 mL sodium acetate buffer (pH = 6.0) and 5 mL pancreatin/amyloglucosidase mixture were added and immediately placed in a 37 °C water bath and shaken. At 0, 10, 20, 30, 60, 90, 120 and 180 min, 1 mL reaction mixture was added to 1 mL anhydrous ethanol, centrifuged (2000 ×*g*, 5 min), and the glucose content of the supernatant was determined using a GOPOD kit. The content of rapidly digestible starch (RDS), slowly digestible starch (SDS), and resistant starch (RS) were calculated using Eqs. (4)–(6):

$$\mathrm{RDS}\ (\%) = 0.9 \times (G_{20} - G_0)/\mathrm{TS} \times 100 \tag{4}$$

$$\mathrm{SDS}\ (\%) = 0.9 \times (G_{120} - G_{20})/\mathrm{TS} \times 100 \tag{5}$$

$$\mathrm{RS}\ (\%) = 0.9 \times (\mathrm{TS} - \mathrm{RDS} - \mathrm{SDS})/\mathrm{TS} \times 100\% \tag{6}$$

where TS is the total starch content of the sample (mg), G_{20} is the glucose content (mg) after 20 min hydrolysis, G_0 is the free glucose content (mg), G_{120} is the glucose content (mg) after 120 min hydrolysis, 0.9 is the glucose conversion factor.

The starch digestion curve was obtained by plotting the starch digestibility (%) as a function of time. According to the first-order kinetic equation of motion (Eq. (7)), the slope logarithm (LOS) analysis method (Eq. (8)) combined with the improved nonlinear least square method (NLLS) was used to fit the digestion rates of all samples.

$$C_t = C_\infty \left[1 - e^{-kt}\right] \tag{7}$$

$$\ln(dC_t/dt) = -kt + \ln(C_\infty - C_0) \tag{8}$$

where C_t represents the starch digestion ratio at a given time (t), C_0 means the starch digestion ratio at the beginning, C_∞ represents the estimated percentage of digested starch after each reaction is completed, and k is the starch digestion rate coefficient.

2.13. Statistical analysis

An analysis of variance (ANOVA) was used to measure statistical differences by the SPSS Version 16.0 software (IBM software, Chicago, USA). Duncan test was used to measure the significant difference ($P <$

0.05). All experiments were carried out at least three times.

3. Results and discussion

3.1. Dynamic rheological properties

The dynamic rheological properties of HBS before and after the addition of HBPs are shown in Fig. 1A-C. The G' and G" reflect the elastic and viscous properties of the gel, respectively. With the increase of angular frequency, G' and G" of all samples showed an increasing trend, and G' was always larger than G", indicating that all HBS gels showed solid-like and cross-linked gel network behavior (Xiao et al., 2022), which was related to the three-dimensional gel network formed by gelatinized starch during the short term retrogradation. The formation of the gel network at this stage was mainly controlled by amylose. The viscoelasticity of gelatinized starch depended on the expansion properties of starch. During the gelatinization process, starch granules absorbed water and expanded, and the amylose was gradually leached out, which increased the effective volume fraction of starch granules, thus increasing G'. Besides, the increase of G' might also be attributed to the aggregation of amylose during the retrogradation process after gelatinization (Xie et al., 2023). Compared with the blank group, the addition of HBPs decreased the G' and G" of the gels, indicating a decrease in viscoelasticity of the HBS/HBPs mixed gels, which indicated that the addition of protein weakened the gel network structure and delayed the short-term retrogradation of starch. On the one hand, the addition of HBPs inhibited the expansion of starch, thus limiting the leaching of amylose. On the other hand, HBPs may interfere with amylose rearrangement through the interaction of its carboxyl group with amylose, resulting in delayed starch retrogradation, which was reflected in the decreased modulus (Tarahi, Hedayati, & Shahidi, 2022). At an angular frequency of 10 rad/s, the samples with the addition of albumin, gliadin and glutenin had similar G' and G" values, while the sample with the addition of globulin had significantly lower G' and G" than them. It was concluded that globulin was most effective in inhibiting HBS short-term retrogradation, which might be due to its lower molecular weight (Fig. S1 and Table S1 in supplementary material) and higher solubility, globulin interacted more effectively with amylose molecules in starch. During the gelatinization and short-term retrogradation of starch, globulin formed complexes or surface coatings with starch molecules, thereby inhibiting starch gelatinization and retrogradation.

As shown in Fig. 1C, the tan δ values of all samples were < 1, indicating that the gels mainly exhibited elastic behavior. With the addition of HBPs, the tan δ values increased, which meant that the three-dimensional gel networks were more weakened. The three-dimensional network structure of the gel was related to the hydrogen bonds formed between starch molecules, and the addition of HBPs broke the balance between hydrophilic and hydrophobic bonds in the original gel system, inhibiting the formation of the gel network structure (Wan et al., 2023). In addition, heat treatment promoted the formation of disulfide bonds between proteins, causing proteins to aggregate and adhere to the surface of starch granules, thus hindering the rearrangement of starch chains, which was also the reason for the decrease of the viscoelastic modulus (Song et al., 2024). Among four HBPs, the final tan δ value for the globulin-added sample was greater than that of the other samples. This may be due to the abundance of free mercaptan (SH) and active disulfide bonds (S—S) in globulin, which can be polymerized by SH oxidation or SH/S-S exchange reactions, and the high tendency of globulin to form polymers *via* disulfide bonds, so globulin more

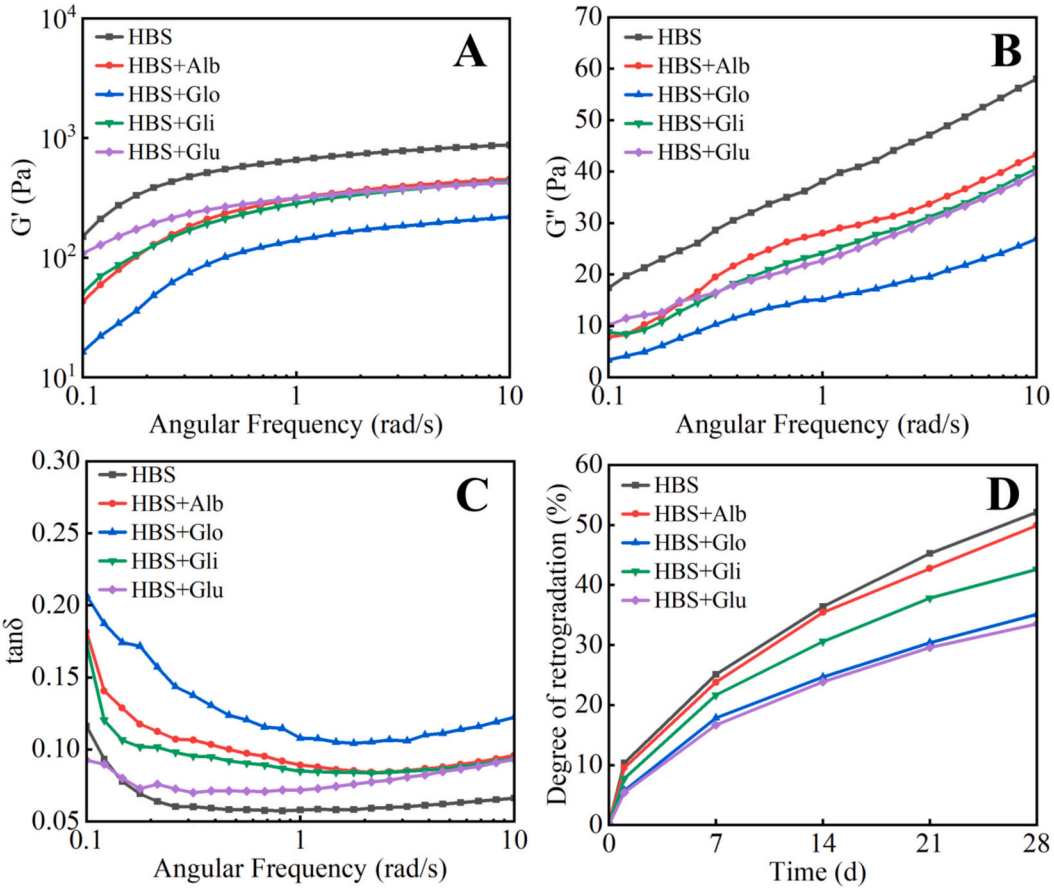

Fig. 1. Changes in the storage moduli (G') (A), the loss modulus (G") (B), tan δ (C) and degree of retrogradation (D) of HBS and HBS/HBPs gels. Alb: albumin; Glo: globulin; Gli: gliadin; Glu: glutenin.

effectively inhibited the rearrangement of starch chains (Zhang et al., 2021).

3.2. Thermal analysis

The gelatinization properties of the samples determined by DSC are shown in Table 1. With the addition of HBPs, the T_O, T_P and T_C of HBS increased significantly, but the ΔH_g decreased significantly, indicating that the addition of four HBPs delayed and inhibited the gelatinization of HBS to varying degrees. This might be because HBPs and starch competed for water molecules, and the presence of HBPs may interfere with the migration of water to starch granules during the heating process, resulting in a reduction in the interaction between starch and water in the mixed system, which reduced the available water for HBS and increased the gelatinization temperature (Lu et al., 2016). In addition, studies have shown that there was an interaction between charged amino acids and starch chains after the addition of proteins, which interfered with solvent interactions and reduced starch granule expansion, leading to an increase in starch gelatinization temperature (Chen, Fang, Federici, Campanella, & Jones, 2020). It could be seen that the addition of globulin significantly increased the T_O, T_P and T_C of HBS, meaning globulin delayed the gelatinization process of HBS, and it was consistent with the explanation in 3.1 (Fig. S1 and Table S1 in supplementary material).

Table 1 shows the change of ΔH_r of the samples stored at 4 °C for 1, 7, 14 and 28 d. The ΔH_r value indicated the degree of recrystallization of starch during the long-term retrogradation, which was related to the slow recombination process of starch molecules during low-temperature storage, reflecting the degree of retrogradation (DR) of starch influenced by the four HBPs (Yang et al., 2021). The ΔH_r values of the samples increased significantly with longer storage time, indicating that the starch recrystallized during storage, requiring more energy to destroy the crystals. Under different storage days, the ΔH_r and DR of the retrograded starch samples with HBPs added were lower than that of the retrograded HBS without HBPs, indicating that all four HBPs could inhibit the long-term retrogradation of HBS, and the inhibition effect on long-term retrogradation was glutenin > globulin > gliadin > albumin. For example, at 28 d of storage, the ΔH_r of HBS without HBPs was 4.34 J/g and the DR was 51.55 % (Fig. 1D), and after addition of albumin, globulin, gliadin and glutenin, the ΔH_r of HBS decreased significantly, and the DR reduced to 48.20 %, 35.06 %, 42.22 % and 32.63 %, respectively. This was because HBPs inhibited the gelatinization of HBS, reducing the fluidity of amylose and amylopectin chains, which limited the recombination of amylopectin at its interface, thereby reducing the recrystallization of starch and the DR (Lu et al., 2016). In addition, the reduction of DR was also attributed to the denaturation of proteins during heating, which exposed hydrophilic groups and hydrophobic amino acids, thus strengthening the interaction between starch and protein, interfering with the formation of hydrogen bonds between starch chains, and resulting in the inhibition of HBS retrogradation (Lu, Ma, Zhan, Wang, & Tian, 2022).

The Avrami model is widely used to study the recrystallization kinetics of starch during the retrogradation process (especially amylopectin) (Zhang et al., 2020). Table 1 lists the Avrami index (n), crystallization rate constant (k) and determination coefficient (R^2). The parameter n is related to crystal nucleation and crystal morphology, and the parameter k is related to crystal growth and crystallization rate. The correlation coefficient R^2 obtained by linear fitting indicates how well the experimental data fit the Avrami model. The n values for all samples were < 1, indicating that starch recrystallisation followed a transient nucleation pattern. Compared with HBS, the crystallization rate constants (k) of starch with the addition of albumin, globulin, gliadin and glutenin were reduced by 3.41 %, 16.10 %, 7.80 % and 18.54 %, respectively, indicating that HBPs could inhibit recrystallization and reduce the retrogradation rate of starch, and the inhibitory effects of different HBPs were consistent with the results of DR. The R^2 of all samples was close to 1 (0.967–0.992), which indicated that the experimental data fit well with the Avrami model. Compared with HBS, the samples with glutenin added had the greatest decrease in k value, followed by globulin, which meant that to achieve the same DR, HBS with glutenin added had the longest storage time, followed by globulin. It has been reported that glutenin was associated with the preferential binding of amylopectin, and that glutenin polypeptides could bind to the outer branch chains of amylopectin to a greater extent through hydrogen bonding, thus interfering with amylopectin nucleation and aggregation (Kuang et al., 2022). Previous studies have shown that globulin can reduce the total water absorption of starch granules in the gelatinization process to inhibit starch gelatinization, thereby inhibiting short-term retrogradation, and thus affecting the long-term retrogradation process of starch, which was also consistent with rheological results (Baxter, Blanchard, & Zhao, 2014). Compared with globulin, glutenin was less soluble in water and had a larger molecular weight (Fig. S1 and Table S1), resulting in a larger number and volume of protein aggregates formed through disulfide bonds, and therefore glutenin was more effective in hindering the rearrangement of starch chains. The weak inhibitory effect of albumin on retrogradation might be attributed to its high-water solubility, which leads to its separation in the phase separation process of retrogradation, thereby affecting its intervention in starch retrogradation.

3.3. LF-NMR analysis

In this study, LF-NMR was used to further analyze the distribution and migration of water in different states of HBS gels during long-term storage. The LF-NMR parameters of the samples stored at 4 °C for a specific time are shown in Table 2, and the spin relaxation time (T_2)

Table 1
Gelatinization temperature and enthalpy value of HBS and HBS/HBPs mixtures; Retrogradation enthalpy (ΔH_r) and Avrami recrystallization kinetic parameters (Avrami) of retrograded HBS and HBS/HBPs gels stored at 4 °C for 1, 7, 14, 21, and 28 d.

Starch sample	Gelatinization parameters				ΔH_r (J/g)					Avrami parameters		
	T_O (°C)	T_P (°C)	T_C (°C)	$\triangle H_g$ (J/g)	1 d	7 d	14 d	21 d	28 d	n	k	R^2
HBS	61.58 ± 0.30^{c}	65.04 ± 0.33^{c}	68.34 ± 0.51^{d}	8.42 ± 0.03^{a}	0.86 ± 0.01^{a}	2.09 ± 0.03^{a}	3.03 ± 0.01^{a}	3.77 ± 0.07^{a}	4.34 ± 0.06^{a}	0.695	0.205	0.972
HBS + Alb	62.42 ± 0.06^{b}	65.89 ± 0.09^{b}	69.03 ± 0.13^{c}	7.49 ± 0.02^{c}	0.69 ± 0.01^{b}	1.72 ± 0.04^{b}	2.56 ± 0.03^{b}	3.09 ± 0.03^{b}	3.61 ± 0.01^{b}	0.704	0.198	0.967
HBS + Glo	64.33 ± 0.12^{a}	68.16 ± 0.11^{a}	71.30 ± 0.16^{a}	7.67 ± 0.09^{b}	0.44 ± 0.06^{d}	1.37 ± 0.03^{d}	1.89 ± 0.01^{d}	2.33 ± 0.04^{d}	2.69 ± 0.03^{d}	0.770	0.172	0.992
HBS + Gli	62.25 ± 0.15^{b}	65.33 ± 0.36^{c}	68.51 ± 0.46^{cd}	7.56 ± 0.05^{c}	0.58 ± 0.03^{c}	1.62 ± 0.03^{c}	2.29 ± 0.01^{c}	2.83 ± 0.03^{c}	3.19 ± 0.03^{c}	0.752	0.189	0.983
HBS + Glu	62.51 ± 0.18^{b}	66.07 ± 0.21^{b}	69.44 ± 0.25^{b}	7.57 ± 0.09^{bc}	0.40 ± 0.04^{d}	1.23 ± 0.01^{e}	1.76 ± 0.06^{e}	2.18 ± 0.11^{d}	2.47 ± 0.01^{e}	0.790	0.167	0.987

Data are expressed as means ± SD of duplicate assays. Values followed by different superscripts in the same column present significantly different ($p < 0.05$). Avrami parameters n, k and R^2 represent Avrami exponent, rate constant and coefficient of determination, respectively. Alb: albumin; Glo: globulin; Gli: gliadin; Glu: glutenin.

Table 2
Relaxation times (ms) and relative percentage of amplitudes (%) of retrograded HBS and HBS/HBPs gels stored at 4 °C for 1, 5, 7, 14, 21, and 28 d.

Storage time	Starch sample	T_2 (ms)			A_2 (%)		
		T_{21}	T_{22}	T_{23}	A_{21}	A_{22}	A_{23}
1 d	HBS	19.37 ± 1.34^{a,A}	594.43 ± 24.10^{a,A}	6150.99 ± 0.00^{A}	0.97 ± 0.08^{d,BC}	97.74 ± 0.06^{c,A}	1.29 ± 0.04^{D}
	HBS + Alb	9.58 ± 1.10^{b,AB}	517.37 ± 20.97^{b,A}	N.D.	1.48 ± 0.05^{c,A}	98.52 ± 0.05^{a,A}	N.D.
	HBS + Glo	7.52 ± 0.81^{c,A,B}	289.94 ± 0.00^{d,A}	N.D.	1.72 ± 0.02^{b,AB}	98.28 ± 0.02^{b,A}	N.D.
	HBS + Gli	9.66 ± 0.00^{b,A}	382.75 ± 0.00^{c,A}	N.D.	1.47 ± 0.09^{c,A}	98.53 ± 0.09^{a,AB}	N.D.
	HBS + Glu	7.49 ± 0.30^{c,A}	310.79 ± 0.00^{d,A}	N.D.	2.16 ± 0.06^{a,AB}	97.84 ± 0.06^{c,A}	N.D.
5 d	HBS	19.43 ± 2.41^{a,A}	567.54 ± 22.48^{a,A}	6488.23 ± 963.72^{A}	1.08 ± 0.06^{e,AB}	97.38 ± 1.00^{b,A}	1.54 ± 0.96^{D}
	HBS + Alb	9.47 ± 0.99^{b,AB}	505.26 ± 0.00^{b,AB}	7593.51 ± 526.33^{A}	1.48 ± 0.09^{c,A}	98.01 ± 0.36^{ab,A}	0.75 ± 0.04^{D}
	HBS + Glo	8.22 ± 0.33^{b,A}	289.94 ± 0.00^{d,A}	N.D.	1.74 ± 0.11^{b,AB}	98.26 ± 0.11^{ab,A}	N.D.
	HBS + Gli	9.67 ± 0.67^{b,A}	382.75 ± 0.00^{c,A}	N.D.	1.32 ± 0.04^{d,B}	98.68 ± 0.04^{a,A}	N.D.
	HBS + Glu	7.50 ± 0.59^{b,A}	276.98 ± 11.23^{d,B}	N.D.	2.24 ± 0.07^{a,A}	97.76 ± 0.08^{ab,A}	N.D.
7 d	HBS	17.64 ± 0.70^{a,A}	554.57 ± 22.48^{a,AB}	5415.74 ± 1033.36^{ab,A}	1.14 ± 0.06^{d,A}	95.11 ± 0.27^{c,B}	3.76 ± 0.31^{a,C}
	HBS + Alb	9.91 ± 0.77^{b,A}	505.26 ± 0.00^{b,AB}	6457.52 ± 1734.14^{a,A}	1.52 ± 0.03^{c,A}	95.90 ± 0.26^{b,B}	2.58 ± 0.28^{b,C}
	HBS + Glo	7.15 ± 0.28^{c,B,C}	276.98 ± 11.23^{d,B}	N.D.	1.84 ± 0.04^{b,A}	98.16 ± 0.04^{a,A}	N.D.
	HBS + Gli	9.67 ± 0.67^{b,AB}	374.19 ± 14.82^{c,A}	3456.47 ± 283.19^{b,A}	1.48 ± 0.11^{c,A}	97.89 ± 0.23^{a,BC}	0.63 ± 0.14^{c,B}
	HBS + Glu	6.84 ± 0.47^{c,A}	270.50 ± 0.00^{d,B}	N.D.	2.19 ± 0.02^{a,A}	97.81 ± 0.02^{a,A}	N.D.
14 d	HBS	18.47 ± 0.75^{a,A}	517.37 ± 20.97^{a,BC}	5066.98 ± 1049.64^{a,A}	1.04 ± 0.04^{d,AB}	94.57 ± 0.12^{d,B}	4.39 ± 0.14^{a,C}
	HBS + Alb	7.96 ± 1.65^{c,BC}	482.67 ± 19.57^{b,B}	3977.39 ± 414.21^{a,B}	1.39 ± 0.08^{c,A}	94.44 ± 0.34^{d,C}	4.17 ± 0.40^{a,B}
	HBS + Glo	7.17 ± 0.59^{c,BC}	258.40 ± 10.47^{d,C}	N.D.	1.62 ± 0.07^{b,B}	98.38 ± 0.07^{a,A}	N.D.
	HBS + Gli	10.15 ± 1.06^{b,A}	374.19 ± 14.82^{c,A}	2614.06 ± 103.54^{b,B}	1.31 ± 0.10^{c,B}	97.42 ± 0.27^{c,C}	1.27 ± 0.17^{b,B}
	HBS + Glu	6.69 ± 0.70^{c,ABC}	241.07 ± 9.77^{d,C}	N.D.	2.10 ± 0.03^{a,B}	97.90 ± 0.02^{b,A}	N.D.
21 d	HBS	14.70 ± 1.19^{a,B}	496.98 ± 20.12^{a,C}	6160.69 ± 744.82^{b,A}	0.89 ± 0.09^{d,CD}	93.51 ± 0.18^{c,C}	5.60 ± 0.27^{a,B}
	HBS + Alb	7.66 ± 0.00^{b,C}	439.76 ± 0.00^{b,C}	3244.90 ± 149.64^{c,B}	1.12 ± 0.11^{c,B}	94.54 ± 0.05^{b,C}	4.33 ± 0.17^{b,B}
	HBS + Glo	6.02 ± 0.49^{c,D}	249.45 ± 0.00^{d,C}	8119.85 ± 0.00^{a}	1.65 ± 0.06^{b,B}	96.34 ± 0.24^{a,B}	2.01 ± 0.29^{c}
	HBS + Gli	7.72 ± 1.12^{b,B}	344.90 ± 0.00^{c,B}	3424.98 ± 162.26^{c,A}	1.25 ± 0.08^{c,B}	94.50 ± 0.38^{b,D}	4.26 ± 0.42^{b,A}
	HBS + Glu	5.71 ± 0.52^{c,C}	230.04 ± 0.00^{e,D}	6920.62 ± 560.08^{b}	1.96 ± 0.00^{a,C}	96.70 ± 0.13^{a,B}	1.34 ± 0.14^{d}
28 d	HBS	14.65 ± 0.00^{a,B}	452.13 ± 21.42^{a,D}	5452.42 ± 793.13^{a,A}	0.79 ± 0.01^{d,D}	90.84 ± 0.83^{b,D}	8.38 ± 0.82^{a,A}
	HBS + Alb	7.27 ± 0.34^{bc,C}	416.95 ± 19.75^{b,C}	2686.15 ± 127.26^{c,B}	1.08 ± 0.08^{c,B}	91.46 ± 0.52^{b,D}	7.46 ± 0.59^{a,A}
	HBS + Glo	6.35 ± 0.29^{bc,CD}	230.04 ± 0.00^{d,D}	6037.94 ± 286.06^{a}	1.46 ± 0.08^{b,C}	94.49 ± 0.32^{a,C}	4.04 ± 0.4^{bc}
	HBS + Gli	7.78 ± 1.57^{b,B}	335.95 ± 15.49^{c,B}	2686.15 ± 127.26^{c,B}	1.04 ± 0.07^{c,C}	94.14 ± 0.82^{a,D}	4.82 ± 0.81^{b,A}
	HBS + Glu	5.87 ± 0.56^{c,BC}	195.64 ± 0.00^{e,E}	4367.02 ± 206.89^{b}	1.82 ± 0.07^{a,D}	95.02 ± 0.38^{a,C}	3.15 ± 0.32^{c}

ND, not detected. Data are expressed as means ± SD of duplicate assays. Different superscript lowercase letters within column indicate statistical significance between averages of different samples retrograded for the same time at $p < 0.05$; different superscript capital letters within column indicate statistical significance between averages of the same sample retrograded for a different time at $p < 0.05$. Alb: albumin; Glo: globulin; Gli: gliadin; Glu: glutenin.

curves of the samples stored at 14 and 28 d are shown in Fig. S2. The T_2 reflects the freedom degree and bonding state of water and is negatively correlated with the binding degree of water molecules (Zhang et al., 2019). The T_2 spectra of the samples had three peaks, in which the corresponding ranges of T_{21} and T_{22} were 5.71–19.43 ms and 195.64–694.43 ms, which represented bound water and free water (physically retained within the starch paste system, thereby reducing its tendency to flow), respectively; the peak of T_{23} was above 1000 ms, which was related to the precipitation of water from the starch in the retrogradation process.

The T_{21} and T_{22} values of all the samples gradually decreased with longer storage time, indicating that the cross-linking of starch molecules further formed a denser gel structure, and the order of the whole system was higher, restricting water mobility (Wu et al., 2023). In addition, the T_{21} and T_{22} values of the HBS/HBPs gels were lower than those of the HBS gel during the retrogradation process, suggesting that the addition of HBPs hindered the free movement of water molecules. This may be because the interaction of HBPs with starch would cause the starch to bind to more water molecules, thus limiting the mobility of water (Yang et al., 2021).

The proportions of the corresponding peak areas of the three peaks were denoted as A_{21}, A_{22}, and A_{23}, respectively (Table 2), representing the relative amounts of water molecules in different degrees of binding. As storage time extended from 1 d to 28 d, the A_{21} and A_{22} values of HBS decreased gradually, while the A_{23} values increased from 1.29 % to 8.38 %. This result was related to the strength of the hydrogen bonds. During the long-term retrogradation process, the hydrogen bonds between the starch chains were strengthened, while the hydrogen bonds between the starch chains and the water molecules were weakened, which reduced the water-holding capacity of the gels and led to water precipitation (Zhang et al., 2020). However, the A_{21} and A_{22} values of the HBS/HBPs gels were always greater than those of HBS and the A_{23} values were always less than those of HBS, which meant that the addition of HBPs could reduce the water loss of the gel. This was because restricted water mobility (decreased T_2) led to reduced recrystallization of the starch chains, which is also a key factor in the inhibition of HBS retrogradation by HBPs.

In addition, T_{23} and A_{23} of samples containing albumin could be detected after 5 d of storage, samples containing gliadin could be detected after 7 d, and samples containing globulin and glutenin could be detected after 21 d, and the A_{23} for globulin was greater than glutenin. These results indicated the ability of HBPs to retain bound water followed the order: glutenin > globulin > gliadin > albumin, which also implied that globulin and glutenin were more effective in inhibiting the long-term retrogradation of HBS. It is worth noting that after 28 d of storage, the A_{23} value of albumin increased more than that of other HBPs and was not significantly different from that of HBS. Combined with the rheological curve in Fig. 1, the G' value of the gel with albumin was slightly lower than that of the HBS gel without the HBPs, which indicated that albumin has certain anti-retrograde properties on HBS, but

mainly play a role in the short-term retrogradation process of HBS. This was because albumin was soluble in water and could compete with starch for water during gelatinization, inhibiting the gelatinization of starch, so the effect of albumin mainly affected the retrogradation in the early stage of storage.

3.4. Hardness analysis

The hardness of starch gel during storage is positively correlated with the degree of retrogradation, so the hardness was usually used as an index to evaluate the degree of retrogradation (Jia et al., 2022). The effect of HBPs on the hardness of HBS gels after 14 and 28 d of storage at 4 °C is shown in Table 3. Obviously, the hardness of HBS gels with or without HBPs both increased with storage time. After storage of 28 d, the hardness of HBS gel increased from 189.46 g to 220.57 g, mainly due to the reordering of amylopectin molecules into a high-density crystalline structure during prolonged refrigeration, resulting in an increase in gel hardness (Zhou et al., 2022). However, compared with HBS, after 14 and 28 d of storage, the texture of HBS/HBPs gels was significantly softer, and the hardness increased at a slower rate, indicating that the addition of HBPs could effectively delay the starch retrogradation. This may be due to the hydrogen bond interactions and entanglement behavior between HBPs and HBS, resulting in higher strength of molecular forces for HBS chain aggregation, under which the recombination between HBS chains was blocked, and the formation of ordered structures (recrystallized structure) were inhibited (Zhu, Zheng, Rao, & Chen, 2023). At 28 d, the hardness of HBS gel supplemented with glutenin was the lowest (147.18 g), which was 33.27 % lower than that of HBS gel without glutenin. This may be because the extended glutenin polypeptide chains after heating contained more β-sheet structures, which meant that glutenin was strongly hydrophobic, resulting in increased connections between glutenin peptide chains and starch chains, thus preventing the starch chains from aggregating during long-term storage (Kuang et al., 2022). In addition, the lower hardness may be due to glutenin giving the gel higher water retention properties, thus making the gel softer, which was consistent with the LF-NMR results.

3.5. XRD analysis

The XRD was used in this study to determine the type and degree of starch crystallization. The XRD patterns of native and gelatinized HBS are shown in Fig. 2A. The pattern of native HBS showed distinct peaks at 15.06°,17.18°, 18.07° and 23.17°, characteristic of an A-type XRD pattern. These characteristic peaks of HBS disappeared after gelatinization without the addition of HBPs. The XRD patterns of HBS/HBPs gel samples stored at 4 °C for 14 and 28 d are shown in Fig. 2B and C. The patterns of all retrograded samples showed two peaks at 17° and 20°, which was consistent with the B + V-type crystalline structure. The B-type crystals mainly resulted from the recrystallization of amylopectin, while V-type crystals formed from the combination of amylose and endogenous lipids (Hou et al., 2020). Compared to 14 d, the intensity of the B-type characteristic peak at 28 d increased, reflecting the aggregation of amylopectin molecules. Moreover, the diffraction peaks of the starch gels still maintained the B + V-type crystalline structure after the addition of HBPs, indicating that the addition of HBPs did not change the crystal type of retrograded starch (Kuang et al., 2022; Wu et al., 2023).

The RC of the retrogradation samples at 14 and 28 d is shown in Table 3. It was clear that the RC of all the samples increased with storage time, where the RC of HBS increased from 11.14 % at 14 d to 13.47 % at 28 d. However, the addition of HBPs decreased the RC of HBS both at 14 and 28 d of storage, indicating that the addition of HBPs inhibited the conversion of starch crystals from an amorphous state to the crystalline state, which mainly depressed the recrystallization of amylopectin (Zhou et al., 2022). This decreasing trend may be due to the incorporation of proteins reducing the probability of collision between starch molecules (Zhang et al., 2019). After 28 d of storage, the RC of retrograded HBS with the addition of albumin, globulin, gliadin and glutenin decreased by 16.59 %, 37.78 %, 29.55 % and 50.80 %, respectively, indicating that HBPs could effectively delay starch retrogradation by inhibiting the recrystallization of amylopectin, among which glutenin had the most significant effect, followed by the globulin. This was due to the interpenetration of the continuous network formed after glutenin hydration in the starch gel matrix, gluten has a large molecular weight and significant steric hindrance, the physical entanglement or non-covalent bonding between glutenin polypeptides and amylopectin, which hindered the interaction between amylopectin (Kuang et al., 2022). This proved that glutenin was indeed block the recrystallization of amylopectin in the amorphous region, which was consistent with the results of the DSC experiments above.

3.6. FTIR analysis

The FTIR technique can be used to monitor changes in various chemical bond types in starch gels. The FTIR spectra of HBS gels stored with or without HBPs for 14 and 28 d are shown in Fig. 2D and E. All samples showed a distinct strong band near 3000–3600 cm^{-1}, related to the stretching vibration of O—H, reflecting the formation of hydrogen bonds (Bai et al., 2024). It was reported that the band around 1650 cm^{-1} may be due to the presence of bound water in the sample and that the band between 800 and 1200 cm^{-1} reflects the presence of crystalline regions, which are also seen as carbohydrate “fingerprint” regions (Anbarani, Razavi, & Taghizadeh, 2021). Compared to 14 d, the bands

Table 3
Variation of hardness, relative crystallinity (RC), R1047/1022, R995/1022 and digestibility parameters of retrograded HBS and HBS/HBPs gels stored at 4 °C for 14 and 28 d.

Storage time	Starch sample	Hardness (g)	RC (%)	R1047/1022	R995/1022	RDS (%)	SDS (%)	RS (%)	C_∞ (%)
14 d	HBS	189.46 ± 3.89^{a}	11.14 ± 0.17^{a}	1.908 ± 0.017^{a}	1.807 ± 0.009^{a}	67.23 ± 0.12^{a}	15.73 ± 0.65^{a}	17.10 ± 0.53^{e}	80.41 ± 2.10^{a}
	HBS + Alb	150.62 ± 3.21^{b}	9.03 ± 0.13^{b}	1.812 ± 0.012^{b}	1.756 ± 0.020^{b}	65.01 ± 1.08^{ab}	15.21 ± 0.98^{a}	19.58 ± 0.11^{d}	77.64 ± 1.99^{a}
	HBS + Glo	140.21 ± 1.22^{c}	7.10 ± 0.17^{cd}	1.630 ± 0.006^{d}	1.508 ± 0.025^{d}	56.44 ± 0.34^{c}	15.05 ± 0.85^{a}	26.34 ± 0.51^{b}	70.64 ± 1.97^{bc}
	HBS + Gli	153.13 ± 2.77^{b}	7.84 ± 0.58^{c}	1.759 ± 0.006^{c}	1.658 ± 0.020^{c}	61.99 ± 2.42^{b}	13.49 ± 1.82^{a}	23.20 ± 0.17^{c}	73.90 ± 1.96^{b}
	HBS + Glu	127.05 ± 0.44^{d}	6.46 ± 0.34^{d}	1.561 ± 0.004^{e}	1.449 ± 0.010^{e}	54.57 ± 0.03^{c}	15.83 ± 0.21^{a}	28.36 ± 0.23^{a}	68.65 ± 2.05^{c}
28 d	HBS	220.57 ± 9.19^{a}	13.47 ± 0.23^{a}	1.978 ± 0.032^{a}	1.866 ± 0.003^{a}	64.85 ± 0.33^{a}	16.05 ± 0.33^{b}	19.16 ± 0.00^{e}	77.92 ± 2.15^{a}
	HBS + Alb	176.08 ± 0.11^{b}	11.24 ± 0.04^{b}	1.879 ± 0.040^{b}	1.809 ± 0.039^{b}	61.28 ± 0.23^{b}	15.86 ± 0.25^{b}	22.91 ± 0.03^{d}	73.99 ± 2.00^{ab}
	HBS + Glo	154.12 ± 1.62^{c}	9.64 ± 0.15^{d}	1.693 ± 0.029^{d}	1.559 ± 0.010^{d}	54.71 ± 0.11^{d}	16.54 ± 0.62^{b}	28.82 ± 0.52^{b}	68.41 ± 2.15^{cd}
	HBS + Gli	180.43 ± 0.06^{b}	10.15 ± 0.25^{c}	1.792 ± 0.007^{c}	1.684 ± 0.016^{c}	58.86 ± 0.28^{c}	14.63 ± 0.24^{c}	26.56 ± 0.04^{c}	71.06 ± 2.25^{bc}
	HBS + Glu	147.18 ± 1.85^{c}	8.58 ± 0.08^{e}	1.611 ± 0.005^{e}	1.504 ± 0.006^{e}	51.82 ± 0.08^{e}	17.64 ± 0.16^{a}	30.61 ± 0.23^{a}	66.17 ± 2.59^{d}

Data are expressed as means ± SD of duplicate assays. Values followed by different superscripts in the same column present significantly different ($p < 0.05$). RDS: rapidly digestible starch, SDS: slowly digestible starch, RS: resistant starch, C_∞: the total starch digested percentage. Alb: albumin; Glo: globulin; Gli: gliadin; Glu: glutenin.

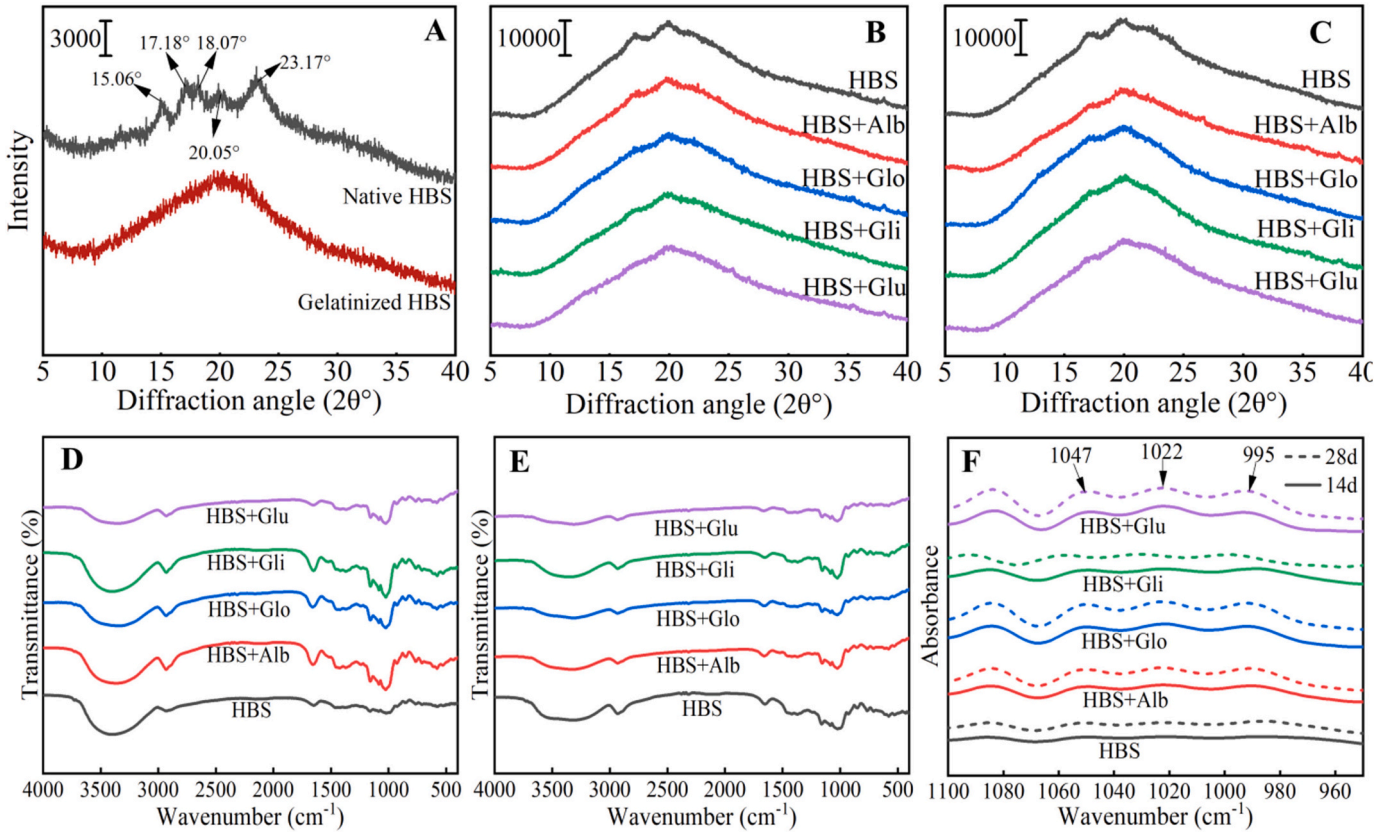

Fig. 2. X-ray diffractograms of native and gelatinization HBS (A) and retrograded HBS and HBS/HBPs gels stored at 4 °C for 14 (B) and 28 d (C). FITR spectra of retrograded HBS and HBS/HBPs gels stored at 4 °C for 14 (D) and 28 d (E) and the deconvoluted FTIR spectra (F). Alb: albumin; Glo: globulin; Gli: gliadin; Glu: glutenin.

in the range of 3000–3600 cm^{-1} were flatter at 28 d for all samples, suggesting that the hydrogen bonding in the sample system had become weaker after 14 d of cryogenic storage (Bai et al., 2024). In addition, after 14 d and 28 d of preservation, the IR absorption bands of the samples with the addition of HBPs were weaker than those of HBS, indicating that the crystalline structures formed were less ordered or more unstable. This was mainly due to the weaker strength and density of hydrogen bonds formed between molecules resulting from HBPs, which led to lower retrogradation rates (Yang, Dhital, Shan, Zhang, & Chen, 2021). Notably, the samples containing glutenin had the weakest IR absorption peaks, indicating a more significant reduction in the hydrogen bonds between starch molecules after the addition of glutenin. The binding of the hydroxyl group of C-6 on the starch molecule to the carbonyl group of tyrosine (Tyr) inhibits retrogradation and the longer chain length of glutenin makes the connection more likely, which leads to a more pronounced suppression of retrogradation (Guo, Lian, Kang, Gao, & Li, 2016).

The FTIR spectra of samples stored for 14 and 28 d were deconvoluted in the 950–1100 cm^{-1} range (Fig. 2F) and intensity ratios of 1047/1022 cm^{-1} and 995/1022 cm^{-1} were calculated to characterize the order and double helix degree of the crystalline regions (Table 3) (An et al., 2024). The values of R1047/1022 and R995/1022 increased with storage time, indicating that the amylopectin molecules had rearranged and the number of ordered structures increased during storage, which meant that the starch gel had retrograded (Zhou et al., 2022). In addition, the R1047/1022 and R995/1022 values of HBS/HBPs gels were significantly lower than those of HBS without HBPs ($p < 0.05$), which demonstrated that the ordered and double helix structures of the crystals reduced, suggesting that the addition of HBPs had an effective inhibition effect on the long-term retrogradation of starch. This can be attributed to the fact that the double helix structure of the short chain branches of amylopectin was unwound during gelatinization, and the protein polypeptide chains could enter the gaps of amylopectin and form hydrogen bonds with the starch, resulting in the weakness of the three-dimensional structure of the gels (Guo, Yang, Wang, Lian, & Liu, 2021).

3.7. SEM analysis

The microscopic morphology of HBS and HBS/HBPs gels at 150 × by SEM is shown in Fig. 3. The water in the gels was removed after freeze-drying, resulting in a porous network structure. The pores of the gel are related to the aggregation of starch molecules and the distribution of water. Compared to samples stored for 14 d, samples stored for 28 d had a smaller pore size and a more compact structure, which was due to the precipitation of water in the gels caused by the rearrangement of amylopectin during long-term storage, resulting in the gels to contract to form an aggregated dense structure (Zhou et al., 2022). In addition, this dense structure was positively correlated with gel strength, which validated the conclusions of hardness analysis.

Apparently, with the addition of HBPs, the gel structures were looser, and the pore sizes were larger, which meant that the presence of HBPs could hinder the above shrinkage phenomenon to a certain extent and make the gels softer. On the one hand, this could be attributed to HBPs retarding water loss and thus increasing the porosity of the gel matrix (Jia et al., 2022). On the other hand, the presence of HBPs induced the formation of more heterogeneous structures, affecting the establishment of a stable network structure of starch gel. It could be observed that the pores of the samples containing gliadin were very uneven. This was due to the insolubility of gliadin in water, which became extremely sticky when heated and adhered to the starch chains, resulting in the structure of the gel network becoming disorganized (Kuang, Ma, Pu, Huang, & Xiong, 2021). At the same time, some of the pore walls in the samples

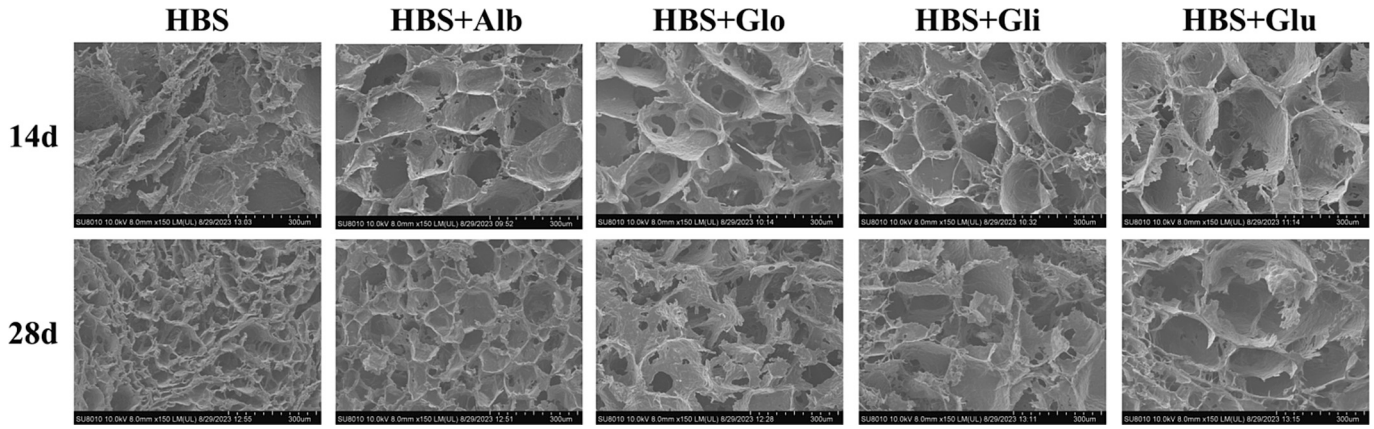

Fig. 3. Scanning electron micrographs of retrograded HBS and HBS/HBPs gels stored at 4 °C for 14 and 28 d. Alb: albumin; Glo: globulin; Gli: gliadin; Glu: glutenin.

with the addition of globulin and glutenin fractured and showed an irregular lamellar structure, which was attributed to the aggregation of proteins during heating/cooling, then randomly dispersed in the gel network (Min et al., 2023). Among them, the breakage of glutenin-added gels was more pronounced, with significant protein aggregation observed in the SEM images on day 28, which may be attributed to the insolubility of glutenin in water and its larger molecular weight compared to globulin (Fig. S1 and Table S1), resulting in a larger number and volume of protein aggregates, thus reducing the stability of the gel network.

3.8. *In vitro digestion*

The RDS, SDS and RS contents of retrograded HBS and HBS/HBPs mixtures stored at 4 °C for 14 and 28 d are shown in Table 3. After 28 d of storage, the RDS content of HBS decreased to 64.85 % from 67.23 % at 14 d of storage, while the RS content increased from 17.10 % to 19.16 %. This suggested that the enzyme sensitivity of retrograded starch is related to storage time. During storage, starch molecules recrystallized, and the larger the crystalline region, the stronger the resistance to enzymatic hydrolysis (Shi & Gao, 2016). In addition, the presence of HBPs significantly reduced the RDS content and increased the RS content of HBS, while the SDS content remained essentially unchanged. Compared with retrograded HBS without protein, the addition of HBPs reduced the RC of HBS (Table 3) but showed higher anti-digestion properties, because the digestion properties of starch not only depended on the crystallinity of retrograded starch but also are related to the mode and site of enzymes action during the interaction between starch and protein. On the one hand, the interaction between HBPs and HBS could block the active site of amylase, thereby reducing the digestibility of HBS (Qiu, Chen, Rao, & Zheng, 2023). On the other hand, the cross-linked protein network bound by disulfide bonds aggregated on starch granules, inhibiting the expansion of starch granules during gelatinization, which caused poor physical accessibility to digestive enzymes, thus increasing the starch's anti-digestive properties (Chen et al., 2019). The RDS content of HBS supplemented with albumin, globulin, gliadin, and glutenin significantly decreased by 5.51 %, 15.64 %, 9.24 % and 20.09 %, respectively ($P < 0.05$) in the retrograded samples at 28 d of storage, suggesting that glutenin was the most effective in inhibiting the digestion of HBS. Glutenin had a large molecular weight (Fig. S1 and Table S1) and significant steric hindrance, making it more difficult for starch molecules to recrystallize during the retrogradation process, which may be the reason for its best anti-digestibility (Kuang et al., 2022).

Digestion plots obtained by enzymatic digestion of all retrograded starch samples using the *in vitro* enzymatic digestion method are shown in Fig. 4 (A, G). They clearly showed an exponential decay shape, characterized by a sharp increase in starch digestion during the first 30 min, followed by a slower digestion phase until the starch digestion reached the maximum level of digestion. This indicated that the digestion process of retrograded HBS followed a first-order kinetics. The model fit curves for all samples measured by the LOS and NLLS methods are shown in Fig. 4 (B—F, H-L), and the C_∞ estimated using the NLLS method are summarized in Table 3. The LOS fits also showed that the digestion rate coefficients in the initial stage were higher than those in the later stage, indicating that the digestibility curves of all samples could be divided into two independent stages. In addition, the percentage of starch at the endpoint (C_∞) decreased for all samples as storage time. The C_∞ order of the retrograded samples stored for 28 d was the highest for HBS (80.32 %), followed by HBS/Alb (77.71 %), HBS/Gli (75.89 %), HBS/Glo (73.34 %) and HBS/Glu (71.60 %). This indicated that the addition of HBPs could effectively slow down the degree of digestion of HBS, which was consistent with the results above.

3.9. *Discussion*

Four different HBPs inhibited the retrogradation of HBS after gelatinization to different degrees. The mechanism is presented in graphical abstract form in Fig. 5. On the one hand, during the gelatinization process, HBPs competed with starch for water molecules, which inhibited starch expansion to a certain extent, and then affected the retrogradation of starch after gelatinization. On the other hand, the interaction between the HBPs and leached amylose in the system could further restrict starch recrystallization. In addition, during heat treatment, protein molecules aggregated on the surface of starch granules, which also inhibited the recombination of starch molecules. The rheological results showed that globulin had the best effect in inhibiting short-term retrogradation. During the long-term retrogradation process, it could be observed from LF-NMR, XRD, FTIR, and SEM results, the addition of HBPs significantly reduced the degree and rate of HBS retrogradation, and the inhibitory effect followed the order: glutenin > globulin > gliadin > albumin. In particular, glutenin showed stronger inhibition of retrogradation due to its ability to form larger protein aggregates and large steric hindrance caused by the high molecular weight. Moreover, RDS and C_∞ in the retrograded HBS with the addition of HBPs were significantly lower compared to the HBS without HBPs, indicating that HBPs significantly reduced the digestibility of HBS, which was related to the interaction between HBPs and HBS blocking the active binding sites of amylase, as well as the aggregation of cross-linked protein networks on the starch granule surface, inhibiting the physical accessibility of digestive enzymes.

4. Conclusion

This study investigated the mechanism by which HBPs enhanced the anti-retrogradation and anti-digestive properties of HBS. An effective

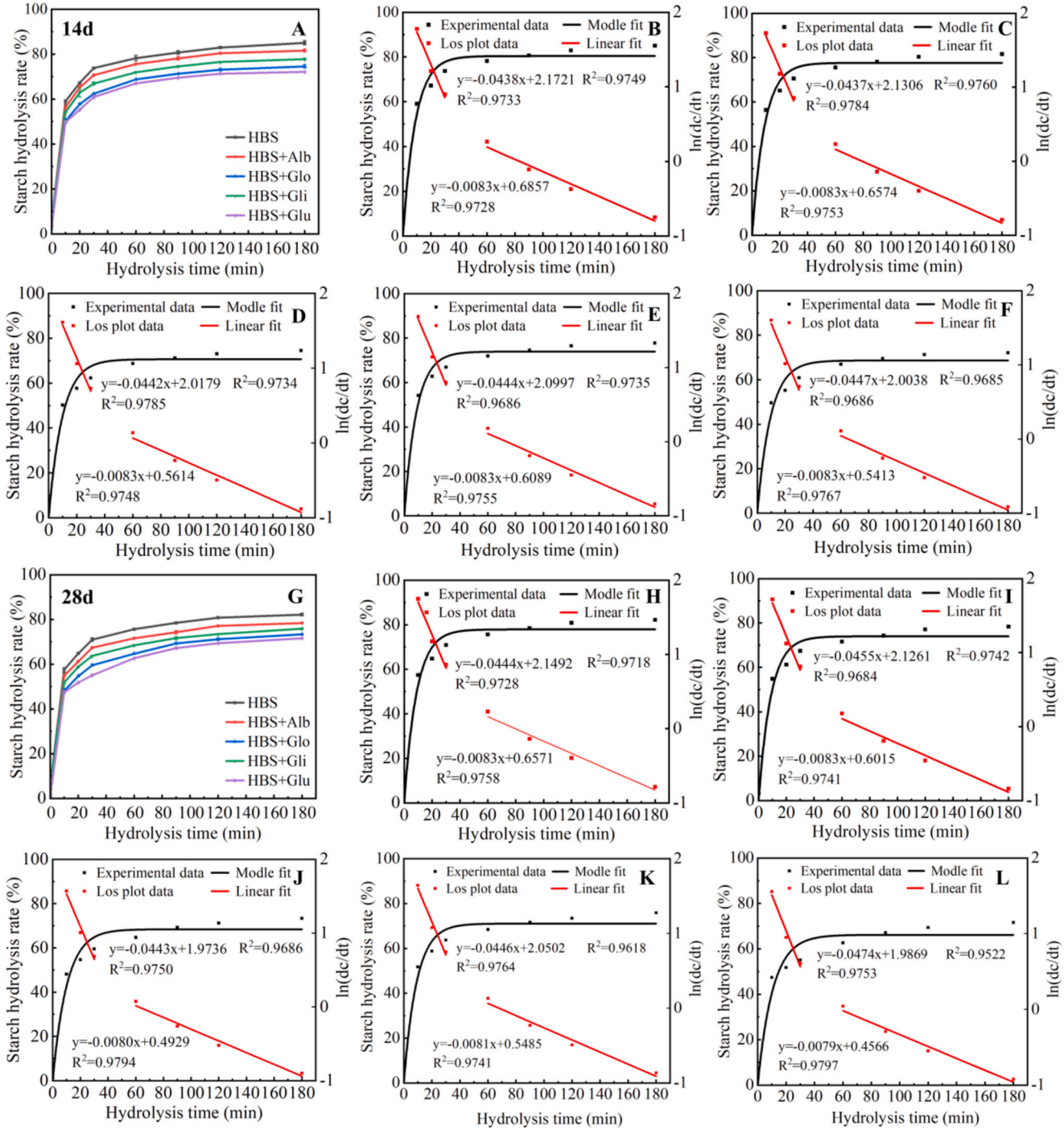

Fig. 4. Digestograms (A and G) and NLLS-fit curves and LOS plots: HBS (B and H), HBS + Alb (C and I), HBS + Glo (D and J), HBS + Gli (E and K), HBS + Glu (F and L) of retrograded HBS and HBS/HBPs gels stored at 4 °C for 14 and 28 d. Alb: albumin; Glo: globulin; Gli: gliadin; Glu: glutenin.

method has been developed to utilize the endogenous proteins in highland barley to modify the properties of HBS. The findings revealed that all four types of HBPs increased the anti-retrogradation properties of HBS by interacting with water molecules and amylose. Specifically, globulin exhibited the highest short-term anti-retrogradation properties, while glutelin showed the highest long-term anti-retrogradation properties. Additionally, the incorporation of HBPs reduced the interaction between amylase and starch, thereby enhancing the anti-digestive properties of HBS. The above results provided basic guidance and relevant data for the development of high-quality nutritional food based on HBS.

CRediT authorship contribution statement

Jiaxin Li: Writing – original draft, Methodology, Data curation, Conceptualization. **Ran Lin:** Writing – original draft, Methodology, Data curation, Conceptualization. **Mengzi Nie:** Methodology, Investigation. **Aixia Wang:** Resources, Methodology. **Xue Gong:** Software, Resources. **Lili Wang:** Resources. **Liya Liu:** Investigation. **Bin Dang:** Conceptualization. **Xijuan Yang:** Investigation. **Fengzhong Wang:** Software, Funding acquisition. **Li-Tao Tong:** Project administration, Funding acquisition.

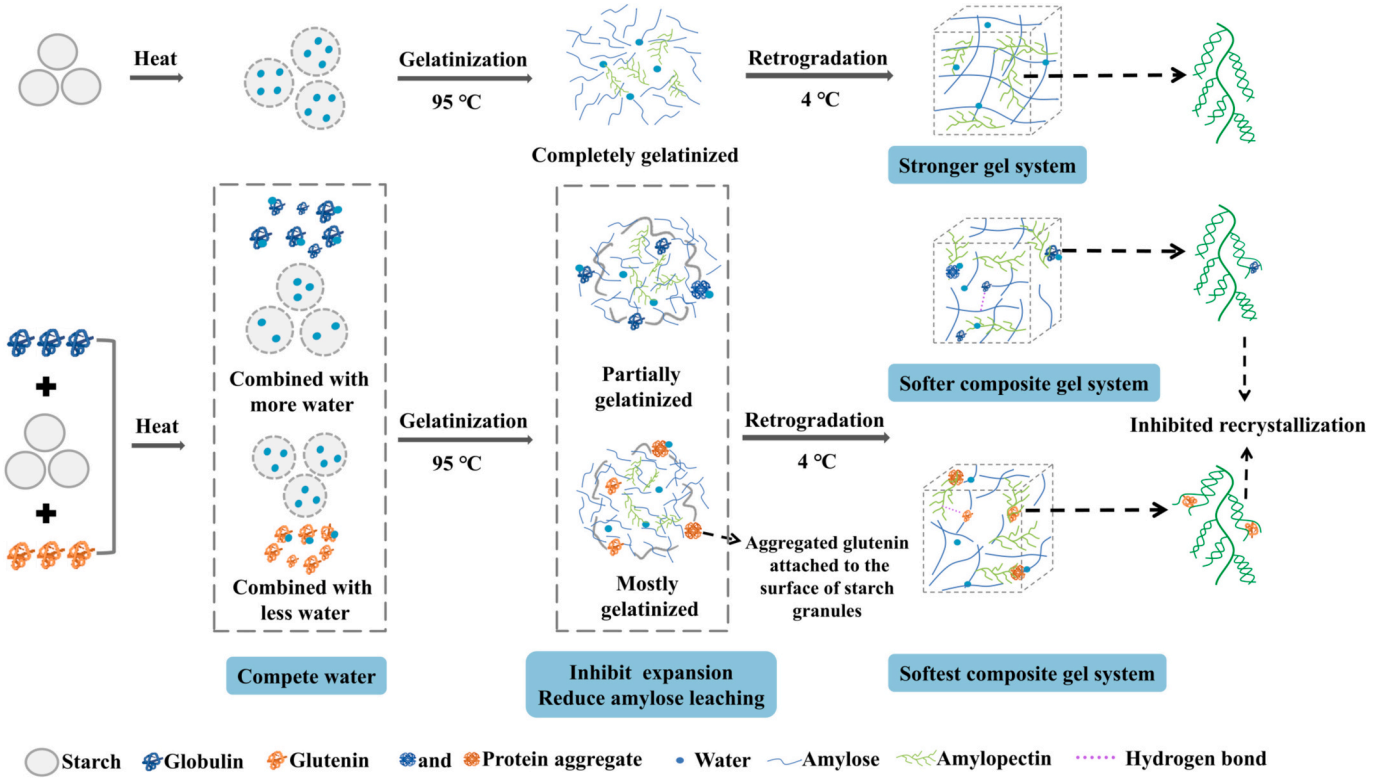

Fig. 5. Graphical Abstract of the mechanisms by which highland barley proteins (HBPs) on the retrogradation characteristics of highland barley starch (HBS).

Declaration of competing interest

The authors confirm that there is no conflict of interest.

Data availability

Data will be made available on request.

Acknowledgements

This study was supported financially by the project of Science and Technology Department of Qinghai Province [2021-NK-A3] and National Natural Science Foundation of China under Grant [31972005].

Appendix A. Supplementary data

Supplementary data to this article can be found online at https://doi.org/10.1016/j.fochx.2024.101915.

References

An, H., Ma, Q., Zhang, F., Zhai, C., Sun, J., Tang, Y., & Wang, W. (2024). Insight into microstructure evolution during starch retrogradation by infrared and Raman spectroscopy combined with two-dimensional correlation spectroscopy analysis. *Food Hydrocolloids, 146, Article 109174*. https://doi.org/10.1016/j.foodhyd.2023.109174

Anbarani, N. M., Razavi, S. M. A., & Taghizadeh, M. (2021). Impact of sage seed gum and whey protein concentrate on the functional properties and retrogradation behavior of native wheat starch gel. *Food Hydrocolloids, 111, Article 106261*. https://doi.org/10.1016/j.foodhyd.2020.106261

Bai, J., Zhang, L., Jia, X., Ye, Q., Pei, J., Song, Q., & Duan, X. (2024). Multi-scale structural changes and mechanistic analysis of wheat starch gels with common proteins in short-term retrogradation at low temperature. *Food Hydrocolloids, 146, Article 109160*. https://doi.org/10.1016/j.foodhyd.2023.109160

Baxter, G., Blanchard, C., & Zhao, J. (2014). Effects of glutelin and globulin on the physicochemical properties of rice starch and flour. *Journal of Cereal Science, 60*(2), 414–420. https://doi.org/10.1016/j.jcs.2014.05.002

Bravo-Nunez, A., Garzon, R., Rosell, C. M., & Gomez, M. (2019). Evaluation of starch(−) protein interactions as a function of pH. *Foods, 8*(5), 155. https://doi.org/10.3390/foods8050155

Chang, Q., Zheng, B., Zhang, Y., & Zeng, H. (2021). A comprehensive review of the factors influencing the formation of retrograded starch. *International Journal of Biological Macromolecules, 186*, 163–173. https://doi.org/10.1016/j.ijbiomac.2021.07.050

Chen, B., Wang, Y. R., Fan, J. L., Yang, Q., & Chen, H. Q. (2019). Effect of glutenin and gliadin modified by protein-glutaminase on retrogradation properties and digestibility of potato starch. *Food Chemistry, 301, Article 125226*. https://doi.org/10.1016/j.foodchem.2019.125226

Chen, D., Fang, F., Federici, E., Campanella, O., & Jones, O. G. (2020). Rheology, microstructure and phase behavior of potato starch-protein fibril mixed gel. *Carbohydrate Polymers, 239*, Article 116247. https://doi.org/10.1016/j.carbpol.2020.116247

Fan, J., Guo, X., & Zhu, K. (2022). Impact of laccase-induced protein cross-linking on the in vitro starch digestion of black highland barley noodles. *Food Hydrocolloids, 124. Article 107298*. https://doi.org/10.1016/j.foodhyd.2021.107298

Gao, M., Hu, Z., Yang, Y., Jin, Z., & Jiao, A. (2024). Effect of different molecular weight β-glucan hydrated with highland barley protein on the quality and in vitro starch digestibility of whole wheat bread. *International Journal of Biological Macromolecules, 268. Article 131681*. https://doi.org/10.1016/j.ijbiomac.2024.131681

Guo, J., Lian, X., Kang, H., Gao, K., & Li, L. (2016). Effects of glutenin in wheat gluten on retrogradation of wheat starch. *European Food Research and Technology, 242*(9), 1485–1494. https://doi.org/10.1007/s00217-016-2649-5

Guo, J., Yang, L., Wang, D., Lian, X., & Liu, C. (2021). Research on the influences of two alcohol soluble glutenins on the retrogradation of wheat amylopectin/amylose. *International Journal of Biological Macromolecules, 183*, 463–472. https://doi.org/10.1016/j.ijbiomac.2021.04.174

Hou, C., Zhao, X., Tian, M., Zhou, Y., Yang, R., Gu, Z., & Wang, P. (2020). Impact of water extractable arabinoxylan with different molecular weight on the gelatinization and retrogradation behavior of wheat starch. *Food Chemistry, 318, Article 126477*. https://doi.org/10.1016/j.foodchem.2020.126477

Jia, Z., Luo, Y., Barba, F. J., Wu, Y., Ding, W., Xiao, S., & Fu, Y. (2022). Effect of beta-cyclodextrins on the physical properties and anti-staling mechanisms of corn starch gels during storage. *Carbohydrate Polymers, 284, Article 119187*. https://doi.org/10.1016/j.carbpol.2022.119187

Khatun, A., Waters, D. L. E., & Liu, L. (2020). The impact of rice protein on in vitro rice starch digestibility. *Food Hydrocolloids, 109, Article 106072*. https://doi.org/10.1016/j.foodhyd.2020.106072

Kong, X.-R., Zhu, Z.-Y., Zhang, X.-J., & Zhu, Y.-M. (2020). Effects of Cordyceps polysaccharides on pasting properties and in vitro starch digestibility of wheat starch. *Food Hydrocolloids, 102, Article 105604*. https://doi.org/10.1016/j.foodhyd.2019.105604

Kuang, J., Huang, J., Ma, W., Min, C., Pu, H., & Xiong, Y. L. (2022). Influence of reconstituted gluten fractions on the short-term and long-term retrogradation of wheat starch. *Food Hydrocolloids, 130, Article 107716*. https://doi.org/10.1016/j.foodhyd.2022.107716

Kuang, J., Ma, W., Pu, H., Huang, J., & Xiong, Y. L. (2021). Control of wheat starch rheological properties and gel structure through modulating granule structure change by reconstituted gluten fractions. *International Journal of Biological Macromolecules, 193*(Pt B), 1707–1715. https://doi.org/10.1016/j.ijbiomac.2021.11.008

Li, L., Pan, F., Tian, X., Li, Y., Rao, L., Zhao, L., & Liao, X. (2024). Assessing the influences of β-glucan on highland barley starch: Insights into gelatinization and molecular interactions. *Food Chemistry, 460, Article 140767*. https://doi.org/10.1016/j.foodchem.2024.140767

Lu, X., Ma, R., Zhan, J., Wang, F., & Tian, Y. (2022). The role of protein and its hydrolysates in regulating the digestive properties of starch: A review. *Trends in Food Science & Technology, 125*, 54–65. https://doi.org/10.1016/j.tifs.2022.04.027

Lu, Z. H., Donner, E., Yada, R. Y., & Liu, Q. (2016). Physicochemical properties and in vitro starch digestibility of potato starch/protein blends. *Carbohydrate Polymers, 154*, 214–222. https://doi.org/10.1016/j.carbpol.2016.08.055

Min, C., Zhang, C., Cao, Y., Li, H., Pu, H., Huang, J., & Xiong, Y. L. (2023). Rheological, textural, and water-immobilizing properties of mung bean starch and flaxseed protein composite gels as potential dysphagia food: The effect of Astragalus polysaccharide. *International Journal of Biological Macromolecules, 239, Article 124236*. https://doi.org/10.1016/j.ijbiomac.2023.124236

Nie, M., Piao, C., Wang, A., Xi, H., Chen, Z., He, Y., & Tong, L. T. (2023). Physicochemical properties and in vitro digestibility of highland barley starch with different extraction methods. *Carbohydrate Polymers, 303*, Article 120458. https://doi.org/10.1016/j.carbpol.2022.120458

Pang, Z., Bourouis, I., Sun, M., Cao, J., Liu, P., Sun, R., & Liu, X. (2022). Physicochemical properties and microstructural behaviors of rice starch/soy proteins mixtures at different proportions. *International Journal of Biological Macromolecules, 209*(Pt B), 2061–2069. https://doi.org/10.1016/j.ijbiomac.2022.04.187

Qiu, Z., Chen, L., Rao, C., & Zheng, B. (2023). Starch-guar gum-ferulic acid molecular interactions alter the ordered structure and ultimate retrogradation properties and in vitro digestibility of chestnut starch under extrusion treatment. *Food Chemistry, 416, Article 135803*. https://doi.org/10.1016/j.foodchem.2023.135803

Shi, M., & Gao, Q. (2016). Recrystallization and in vitro digestibility of wrinkled pea starch gel by temperature cycling. *Food Hydrocolloids, 61*, 712–719. https://doi.org/10.1016/j.foodhyd.2016.06.033

Song, B., Xu, X., Hou, J., Liu, M., Yi, N., Zhao, C., & Liu, J. (2024). Research on corn starch and black bean protein isolate interactions during gelatinization and their effects on physicochemical properties of the blends. *International Journal of Biological Macromolecules, 254, Article 127827*. https://doi.org/10.1016/j.ijbiomac.2023.127827

Tarahi, M., Hedayati, S., & Shahidi, F. (2022). Effects of mung bean (Vigna radiata) protein isolate on rheological, textural, and structural properties of native corn starch. *Polymers, 14*(15). https://doi.org/10.3390/polym14153012

Tavano, O. L., Amista, M. J. M., Del Ciello, G., Rodrigues, M. C. M., Bono Nishida, A. M., Valadares, L. A., & Silva Junior, S. I. D. (2022). Isolation and evaluation of quinoa (Chenopodium quinoa Willd.) protein fractions. A nutritional and bio-functional approach to the globulin fraction. *Current Research in Food Science, 5*, 1028–1037. https://doi.org/10.1016/j.crfs.2022.06.006

Wan, L., Wang, X., Liu, H., Xiao, S., Ding, W., Pan, X., & Fu, Y. (2023). Retrogradation inhibition of wheat starch with wheat oligopeptides. *Food Chemistry, 427, Article 136723*. https://doi.org/10.1016/j.foodchem.2023.136723

Wu, C., Gong, X., Zhang, J., Zhang, C., Qian, J. Y., & Zhu, W. (2023). Effect of rice protein on the gelatinization and retrogradation properties of rice starch. *International Journal of Biological Macromolecules, 242(Pt 3), Article 125061*. https://doi.org/10.1016/j.ijbiomac.2023.125061

Xiao, W., Shen, M., Ren, Y., Wen, H., Li, J., Rong, L., & Xie, J. (2022). Controlling the pasting, rheological, gel, and structural properties of corn starch by incorporation of debranched waxy corn starch. *Food Hydrocolloids, 123, Article 107136*. https://doi.org/10.1016/j.foodhyd.2021.107136

Xie, Q., Liu, X., Liu, H., Zhang, Y., Xiao, S., Ding, W., & Wang, X. (2023). Insight into the effect of garlic peptides on the physicochemical and anti-staling properties of wheat starch. *International Journal of Biological Macromolecules, 229*, 363–371. https://doi.org/10.1016/j.ijbiomac.2022.12.253

Yang, C., Zhong, F., Douglas Goff, H., & Li, Y. (2019). Study on starch-protein interactions and their effects on physicochemical and digestible properties of the blends. *Food Chemistry, 280*, 51–58. https://doi.org/10.1016/j.foodchem.2018.12.028

Yang, H., Tang, M., Wu, W., Ding, W., Ding, B., & Wang, X. (2021). Study on inhibition effects and mechanism of wheat starch retrogradation by polyols. *Food Hydrocolloids, 121, Article 106996*. https://doi.org/10.1016/j.foodhyd.2021.106996

Yang, S., Dhital, S., Shan, C.-S., Zhang, M.-N., & Chen, Z.-G. (2021). Ordered structural changes of retrograded starch gel over long-term storage in wet starch noodles. *Carbohydrate Polymers, 270, Article 118367*. https://doi.org/10.1016/j.carbpol.2021.118367

Yang, Y., Wang, Y., Zhang, R., Jiao, A., & Jin, Z. (2024). The impact of different soluble endogenous proteins and their combinations with β-glucan on the in vitro digestibility, microstructure, and physicochemical properties of highland barley starch. *International Journal of Biological Macromolecules, 260, Article 129417*. https://doi.org/10.1016/j.ijbiomac.2024.129417

Yang, Z., McClements, D. J., Xu, Z., Meng, M., Li, C., Chen, L., & Jin, Z. (2022). Carbohydrate-based functional ingredients derived from starch: Current status and future prospects. *Food Hydrocolloids, 131, Article 107729*. https://doi.org/10.1016/j.foodhyd.2022.107729

Zhang, D., Lin, Z., Lei, W., & Zhong, G. (2020). Synergistic effects of acetylated distarch adipate and sesbania gum on gelatinization and retrogradation of wheat starch. *International Journal of Biological Macromolecules, 156*, 171–179. https://doi.org/10.1016/j.ijbiomac.2020.03.256

Zhang, L.-L., Guan, E.-Q., Yang, Y.-L., Liu, Y.-X., Zhang, T.-J., & Bian, K. (2021). Impact of wheat globulin addition on dough rheological properties and quality of cooked noodles. *Food Chemistry, 362, Article 130170*. https://doi.org/10.1016/j.foodchem.2021.130170

Zhang, M., Sun, C., Wang, X., Wang, N., & Zhou, Y. (2020). Effect of rice protein hydrolysates on the short-term and long-term retrogradation of wheat starch. *International Journal of Biological Macromolecules, 155*, 1169–1175. https://doi.org/10.1016/j.ijbiomac.2019.11.084

Zhang, Y., Chen, C., Chen, Y., & Chen, Y. (2019). Effect of rice protein on the water mobility, water migration and microstructure of rice starch during retrogradation. *Food Hydrocolloids, 91*, 136–142. https://doi.org/10.1016/j.foodhyd.2019.01.015

Zhou, J., Jia, Z., Wang, M., Wang, Q., Barba, F. J., Wan, L., & Fu, Y. (2022). Effects of Laminaria japonica polysaccharides on gelatinization properties and long-term retrogradation of wheat starch. *Food Hydrocolloids, 133, Article 107908*. https://doi.org/10.1016/j.foodhyd.2022.107908

Zhu, F. (2017). Barley starch: Composition, structure, properties, and modifications. *Comprehensive Reviews in Food Science and Food Safety, 16*(4), 558–579. https://doi.org/10.1111/1541-4337.12265

Zhu, J., Zheng, B., Rao, C., & Chen, L. (2023). Effect of extrusion with hydrocolloid-starch molecular interactions on retrogradation and in vitro digestibility of chestnut starch and processing properties of chestnut flour. *Food Hydrocolloids, 140, Article 108633*. https://doi.org/10.1016/j.foodhyd.2023.108633